A Divalent Metal Ion Binding Site in the Kinase Insert Domain of the α-Platelet-Derived Growth Factor Receptor Regulates Its Association with SH2 Domains†

Daruka Mahadevan,‡ Narmada Thanki,§ Pilar Aroca,‡ Peter McPhie,|| Jin-Chen Yu,‡ John Beeler,‡ Eugenio Santos,‡ Alexander Wlodawer,§ and Mohammad A. Heidaran*,‡

Laboratory of Cellular and Molecular Biology, National Cancer Institute, National Institutes of Health, 9000 Rockville Pike, Bethesda, Maryland 20892, Macromolecular Structure Laboratory, NCI−FCRDC, ABL−Basic Research Program, P.O. Box B, Frederick, Maryland 21702, and Laboratory of Biochemistry and Metabolism, NIDDK, 9000 Rockville Pike, Bethesda, Maryland 20982

Received July 29, 1994; Revised Manuscript Received October 5, 1994⊗

ABSTRACT: To investigate the effects of metal ion binding to the α-PDGFR kinase insert domain, a PCR product representing amino acid residues 691−795 (104 amino acids) was bacterially expressed and purified. Secondary structure prediction and circular dichroism spectroscopy indicated this domain to be a mixed α+β protein with a large coil/turn contribution. This 16 kDa, soluble, nonphosphorylated domain bound to $^{45}Ca^{2+}$ and $^{65}Zn^{2+}$ through a common shared site. Of the unlabeled divalent and trivalent metal ions tested, $Ho^{3+} = Zn^{2+} > Ni^{2+} > Ca^{2+} = Mn^{2+} > Mg^{2+}$, Ba^{2+} in competing for $^{45}Ca^{2+}$ binding to this domain. In the presence of Ca^{2+} ions, the conformation of the KI domain changed significantly, and this changed conformation was resistant to subtilisin proteolysis. However, in the presence of Zn^{2+} ions, the conformation of the KI domain changed only slightly. Nevertheless, Zn^{2+} ions were more effective in rendering the KI domain resistant to proteolysis as compared to that shown by Ca^{2+} ions. *In vitro* binding studies using purified baculovirus-expressed α-PDGFR showed a marked increase in binding the p85 N-SH2 domain in the presence of Ca^{2+} or Zn^{2+} ions (K_D = 0.5 μM), suggesting that metal ion binding enhances association of the p85 N-SH2 domain with the receptor. To confirm this, association of the α-PDGFR with the p85 N-SH2 domain was tested in the presence of the KI domain. The nonphosphorylated KI domain was effective in competing with the α-PDGFR for the binding of the p85 N-SH2 domain. This effect was more pronounced in the presence of Ca^{2+} ions. Microinjection of this domain into *Xenopus* oocytes delayed maturation in the presence of insulin but not progesterone. This suggests that the KI domain has a correctly folded three-dimensional structure compatible with biological activity. Together these findings indicate that the recombinant α-PDGFR KI domain binds the p85 N-SH2 domain and this binding is modulated by the presence of a novel divalent metal ion binding site within its structure.

Platelet-derived growth factor (PDGF),[1] a disulfide-linked dimer, is a potent mitogen for cells of mesenchymal origin. Two isoforms, expressed by distinct genes, form homodimers (AA and BB) and a heterodimer (AB), which differentially bind and activate two receptor isoforms (α-PDGFR and β-PDGFR). The high-affinity binding of PDGF to its receptor leads to receptor dimerization, tyrosine kinase activation, and trans autophosphorylation of the receptor on specific tyrosine residues [for a review, see Heldin (1992)]. The phosphorylated receptor is a target for binding Src-homology region 2 (SH2) domains present on a number of intracellular signal transduction proteins, which includes phosphatidylinositol 3-kinase (PI-3K), GTPase activating protein (GAP), and phospholipase C_γ (PLC_γ) (Koch et al., 1991; Cantley et al., 1991; Ullrich & Schlessinger, 1990). These enzymes in turn activate downstream signaling pathways which eventually lead to changes in cell metabolism, architecture, and proliferation.

The PDGFR belongs to a class of receptors which possess immunoglobulin-like extracellular domains, a single membrane-spanning region, and an intracellular tyrosine kinase domain (Yarden et al., 1986; Heldin & Westermark, 1990). The tyrosine kinases like the serine/threonine kinases possess two domains, a smaller N-terminal β-sheet domain and a larger α-helical C-terminal domain with the active site residing between the two domains (Knighton et al., 1991a,b; Bossemeyer et al., 1993). For the PDGFR subfamily which includes the colony stimulating factor-1 receptor (CSF-1R) (c-fms), flt, and c-kit, a kinase insert domain of variable length (76−100 residues) is positioned at the beginning of the C-terminal α-helical domain, thus interrupting the two-domain kinase (Yarden et al., 1986; Hanks & Quinn, 1991). Specific tyrosine residues within this kinase insert domain (KI) become phosphorylated on receptor activation, and these phosphorylated tyrosines bind the SH2 domains of PI-3K

† This research was sponsored in part by the National Cancer Institute, DHHS, under Contract N01-CO-74101 with ABL. D.M. is a Fogarty International Fellow.

* Corresponding author. Telephone: (301) 496-9464. Fax: (301) 496-8479.

‡ Laboratory of Cellular and Molecular Biology, National Cancer Institute.

§ ABL−Basic Research Program.

|| Laboratory of Biochemistry and Metabolism, NIDDK.

⊗ Abstract published in *Advance ACS Abstracts,* January 15, 1995.

[1] Abbreviations: PI-3K, phosphatidylinositol 3-kinase; α-PDGFR, α-platelet-derived growth factor receptor; KI, kinase insert; SH2, Src-homology region 2; CSF-1R, colony stimulating factor-1 receptor; GAP, GTPase activating protein; IRS-1, insulin receptor substrate-1; CD, circular dichroism.

This article not subject to U.S. Copyright. Published 1995 by the American Chemical Society

(p85) and GAP. For example, Tyr731 and Tyr742 of the human α-PDGFR and Tyr740 and Tyr751 of the human β-PDGFR bind the SH2 domains of PI-3K (p85) (Yu et al., 1991; Fantl et al., 1992; Kashishian et al., 1992). The latter also binds the CSF-1R on Tyr721 (Shurtleff et al., 1990). However, the SH2 domains of GAP bind Tyr771 of the β-PDGFR (Fantl et al., 1992; Kashishian et al., 1992). In contrast, the binding of GAP to the α-PDGFR is absent (Bazenet & Kazlaukas, 1993) or of lower affinity (Heidaran et al., 1993).

The presence of a binding domain within the tyrosine kinase domain may have a functional advantage for the PDGFR subfamily. This aspect has been studied by deletion and substitution mutagenesis of the KI domains of the PDGFRs and the CSF-1R (Escobedo & Williams, 1988; Taylor et al., 1989; Morrison et al., 1990; Heidaran et al., 1991). For the PDGFRs, deletion of 80% of the KI domain resulted in inability of the receptor to associate with PI-3K and GAP. These receptors were also defective in transducing the mitogenic signal in response to PDGF. A larger deletion of 95% of the KI domain decreased or abolished biochemical responses (Severinsson et al., 1990; Heidaran et al., 1991). However, signaling through the α-PDGFR was restored when the KI domain of the CSF-1R was inserted into the larger deletion mutant (Heidaran et al., 1991). Recent substitution mutagenesis experiments with the β-PDGFR, in which the tyrosines that bind PI-3 kinase (740, 751), PLC$_\gamma$ (1009, 1021), and GAP (771) were mutated to phenylalanines, produced an inactive receptor. However, when the tyrosines that bind PI-3 kinase or PLC$_\gamma$ were reintroduced into the PDGFR, mitogenic signaling was restored (Valius & Kazlaukas, 1993). Other studies have also shown that PI-3K is required for PDGFR trafficking (Joly et al., 1994) and chemotaxis (Wennstrom et al., 1994; Kundra et al., 1994).

In this paper, we show that the α-PDGFR KI domain contains a novel divalent cation binding site that may be essential for the recognition of the PI-3K (p85) N-terminal SH2 (N-SH2) domain. The association of the p85 N-SH2 domain with the α-PDGFR was markedly enhanced in the presence of divalent cations, suggesting the importance of these cations in receptor-mediated signal transduction. *In vitro*, the KI domain effectively competed with the α-PDGFR for binding the N-SH2 domain of PI-3K (p85), and this effect was markedly increased in the presence of calcium ions.

MATERIALS AND METHODS

Cloning Strategy, Bacterial Expression, and Protein Purification. The DNA sequence corresponding to the human α-PDGFR kinase insert (KI) domain (residues 691−795) was synthesized using the polymerase chain reaction (PCR) method with a *Bam*HI and a *Hin*dIII site at the respective 5′ and 3′ ends. The DNA fragment was cloned into a pQE9 plasmid (type 4) containing a six histidine N-terminal tag (Qiagen). DNA sequencing confirmed the authenticity of the insert. The pQE9 plasmid containing the KI DNA was transformed into competent *Escherichia coli* M15 cells carrying the plasmid pREP4. Expression of the recombinant KI domain was induced with 1.0 mM IPTG (isopropyl β-D-thiogalactopyranoside) once the optical density of the culture reached 0.7 at 600 nm. After 4 h, cells were pelleted and frozen at −70 °C. Protein purification was performed by solubilizing the pellet in 6 M guanidine hydrochloride in 100 mM phosphate/10 mM Tris buffer at pH 8.0. The lysate was then loaded onto a Ni^{2+}-chelate affinity column. The pass-through was reloaded once, and the column was washed with 8 M urea in 100 mM phosphate/10 mM Tris, pH 8.0 and 6.3, to remove bacterial proteins. The KI domain was then eluted with the urea buffer at pH 5.9 and 4.5. Protein was checked spectrophotometrically at 280 nm and 14% SDS−PAGE analysis. The protein was refolded in urea step gradients into either 10 mM Tris-HCl buffer at pH 7.0 or 50 mM phosphate buffer at pH 7.0. The protein was further purified by FPLC (Mono Q) (Pharmacia) and concentrated using Centricon 3 membranes (Amicon).

Stains-all Binding to the Native KI Domain in Aqueous Solution. The interaction of Stains-all, a cationic carbocyanine dye, with the KI domain, vitamin D dependent calcium binding protein (CaBP) (Sigma), and albumin (Sigma) was studied in aqueous solution. The standard solution contained 10 mM Tris base, pH 8.8, 0.001% Stains-all, and 0.1% formamide. The above proteins in 10 mM Tris buffer, pH 7.0 at a concentration of 10 μg, were added to 1.0 mL of solution and then incubated at room temperature in the dark for 30 min. The absorbance in the range 550−700 nm was measured against a control solution, containing no protein using a U-2000 Hitachi spectrophotometer.

$^{45}Ca^{2+}$ and $^{65}Zn^{2+}$ Overlay Study. The detection of Ca^{2+} and Zn^{2+} binding to the highly purified, recombinant α-PDGFR KI domain was carried out as described by Maruyama et al. (1984) and modified according to Kawasaki et al. (1985). The protein at 2.5 μg concentration was bound to nitrocellulose membranes via the Mini Fold II Slot Blot System (Schleicher & Schuell Incorporated, Keene, NH). The filters were washed twice for 10 min at room temperature with overlay buffer (10 mM imidazole, pH 6.8, 100 mM NaCl) (Gailit & Ruoslahti, 1988) containing 10 mM EDTA to remove any protein-bound cations. The filters were then washed 4 times with overlay buffer to remove the EDTA. The $^{45}Ca^{2+}$ (Amersham) overlay was performed by incubating the filters for 30 min at room temperature in overlay buffer containing 0.44 μCi/mL (5 μL in 2 mL) of 50 nM $^{45}Ca^{2+}$ in the absence or presence of 0.5 mM unlabeled dichloride forms of other cations and the trivalent lanthanide holmium chloride. The filters were rapidly rinsed with 50% ethanol in water, air-dried, and exposed to Kodak XAR-5 X-ray film for 24 h at room temperature. Titration of the calcium effect was performed as described above with increasing concentrations of unlabeled calcium ions (0.1−5.0 mM). The $^{45}Ca^{2+}$ overlay was also carried out for vitamin D dependent calcium protein (CaBP) (2.5 μg) and the N-terminal SH2 domain of GAP (2.5 μg). For quantitative analysis, the filters were exposed onto a phosphor screen and analyzed by using a Phosphoimager (Molecular Dynamics).

Since the recombinant KI domain was synthesized with a six-histidine N-terminal tag, these histidines were modified with a saturating concentration of diethyl pyrocarbonate (DEPC) at 240 mM in 2% v/v ethanol in water. The above procedure described for $^{45}Ca^{2+}$ was repeated with 50 nM $^{65}Zn^{2+}$ (0.5 μCi/mL, 2 μL/2 mL) and unlabeled $ZnCl_2$ (0.5−50 μM). The data were quantified as described above.

Circular Dichroism Spectroscopy. The CD spectrum (far-UV 190−260 nm) of the KI domain (0.1 mg/mL) was recorded at 22 °C with a JASCO J-500C spectropolarimeter, using a 1 mm demountable "strain free" quartz cuvette. The following settings were used: bandwidth, 1 nm; time constant, 2.0 s; step resolution, 0.1 nm; scan speed, 10 mdeg/

min; sensitivity, 1 mdeg/cm. Each spectrum represents an average of four scans with the base line subtracted. CD studies were conducted in 10 mM Tris-HCl, pH 7.0. Calcium chloride or zinc chloride was added in varying amounts (1−100 μM). The recorded spectra are presented in terms of molar ellipticity based on a mean residue weight of 110. Secondary structure analysis was performed using the method of Chang et al. (1978).

Subtilisin Proteolysis Susceptibility Assay. Proteolysis with subtilisin was performed in 10 mM Tris-HCl buffer at pH 7.0. The protein concentration was 0.1 mg/mL. Various amounts of calcium chloride (0.1−5.0 mM) and zinc chloride (0.01−2.0 mM) were added, followed by subtilisin at a concentration at 1 μg/mL. Digestion (after 5 and 10 min at 37 °C) was terminated by the addition of double-strength sample buffer containing 20 mM EDTA and 1% 2-mercaptoethanol, followed by immediate heating to 100 °C for 5 min. Samples were analyzed on SDS, 14% PAGE and stained with Coomassie blue. The protease-resistant material was quantified by scanning on a Bio-Rad 620 video densitometer, and the data were analyzed using the 1-D analyst package.

Binding Analysis of the p85 N-SH2 Domain to Purified α-PDGFR. Baculovirus-expressed purified human α-PDGFR (Jensen et al., 1992), in the absence of ATP, Mg^{2+}, and Mn^{2+}, was used to probe the purified p85 N-SH2 domain (2.5 μg) on a nitrocellulose filter using the Slot-Blot method described above. The purification of the p85 N-SH2 domain is described elsewhere (Mahadevan et al., 1994). Nonspecific binding was blocked by treating the membranes with 3% nonfat dry milk in TTBS (25 mM Tris, pH 7.4, 150 mM NaCl, and 0.05% Tween 20) for 1 h. To measure *in vitro* association of the PDGFRs with the p85 N-SH2 domain, membranes were incubated with 5 mL of binding assay buffer (50 mM Hepes, pH 7.4, 0.01% Triton X-100) including 50 ng of purified PDGFRs for 2 h at 25 °C. Binding assays were also performed in the presence of 0.1−10 μM $ZnCl_2$. Membranes were washed twice and then blotted with anti-phosphotyrosine antibodies (UBI). After overnight incubation, membranes were washed twice, probed with ^{125}I-protein A, washed again 4 times in TTBS, and then autoradiographed by exposure of Kodak Xar-5 X-ray film. The autoradiograms were quantified by scanning on a Bio-Rad 620 video denistometer, and the data were analyzed using the 1-D analyst package.

In Vitro Competition Assay of the N-SH2 Domain of p85 (PI-3K) with Purified α-PDGFR and the KI Domain. The purified N-SH2 domain of p85 (PI-3K) at a concentration of 2.5 μg was bound to nitrocellulose membranes via the Mini Fold II Slot Blot system. The filters were washed twice for 10 min at room temperature with overlay buffer (25 mM Tris, pH 7.4, 150 mM NaCl) containing 10 mM EDTA to remove any protein-bound cations (Gailit & Rouslahti, 1988). The filters were washed 4 times with binding buffer (50 mM Hepes, pH 7.0, 50 mM NaCl, and 0.1% Triton X-100) to remove the EDTA. To measure the *in vitro* association of the PDGFR with the N-SH2 domain of p85, the filters were incubated with 5 mL of binding buffer including 50 ng of purified PDGFR for 2 h at room temperature. For the competition assay, the KI domain at different concentrations (0.1−14 μM) in the absence or presence of 0.5 mM $CaCl_2$ was added and incubated for 2 h at room temperature. The filters were then washed twice with binding buffer and blotted with anti-phosphotyrosine antibodies (UBI), for 2 h at room temperature. The filters were washed twice and probed with ^{125}I-protein A, washed again 4 times with binding buffer, air-dried, and exposed to Kodak XAR-5 X-ray film for 24 h at −70 °C. The procedure was repeated with two hexapeptides, DYMDMK and QYVPML (phosphorylated and nonphosphorylated on the tyrosine), from the KI domain of the α-PDGFR which are consensus peptides that bind the SH2 domains of p85. The peptides were used in combination at a concentration of 4 and 40 μM. The data were quantified as described above.

Oocyte Preparation and Microinjection. Adult female *Xenopus laevis* were obtained from Nasco (Fort Atkinson, WI). Ovarian fragments were surgically removed from gonadotropin-stimulated animals anesthezized by hypothermia. Fully grown stage VI oocytes were manually dissected into ND-96 medium (5 mM Hepes, 96 mM NaCl, 1 mM $MgCl_2$, 2 mM KCl, 1.8 mM $CaCl_2$, pH 7.8, and 10 μg/mL each of penicillin and streptomycin sulfate). The oocytes were allowed to recover overnight in the same buffer and were maintained at 20 °C. For induction of meiotic maturation, groups of 15−20 oocytes incubated in ND-96 medium without KCl in the presence of 7 μM insulin (Sigma) or 15 μM progesterone (Sigma) were microinjected with 60 nL of α-PDGFR KI domain in 20 mM Tris-HCl, pH 7.5, reaching a final concentration of 90 ng of this domain in the oocyte. Meiotic maturation was assayed by scoring the disappearance of the nucleus (GVBD) from the oocytes. The above experiments were repeated with the tyrosine phosphorylated and nonphosphorylated hexapeptides and the colony stimulating factor-1 receptor (CSF-1R) KI domain at a final concentration of 90 ng.

Sequence Alignments and Secondary Structure Prediction. The KI domains from the human and mouse α- and β-PDGFR, human CSF-1R (c-fms), fms-like receptor (flt), and c-kit were visually aligned with insertions and deletions to optimize sequence similarity. For each sequence, a joint secondary structure prediction was obtained, using the Leeds Secondary Structure Prediction Suite of Programs, version 3 (Eliopoulos et al., 1982), running on a Vax computer. The eight prediction methods employed by the Leeds suite are those of Nagano (1973), Chou and Fasman (1974), Lim (1974), MacLachlan (1974, unpublished), Burgess et al. (1974), Dufton and Hider (1977), and Garnier et al. (1978). The predictions at each residue in the sequence are summed up to produce a joint result. When appropriate, insertions, deletions, and special sequences (e.g., proline and glycine) were used as parsing points to modify the joint prediction to distinguish turn/loop regions from regular secondary structure. An average prediction of secondary structural elements from the above sequences was ascertained visually.

Prediction of Calcium and Zinc Binding Sites within the α-PDGFR KI Domain. The α-PDGFR KI domain sequence was examined with the other KI domains (see above) for a conserved arrangement of clustered oxygen ligands that could bind calcium ions. Known calcium binding sequences (Kretsinger, 1980; Vyas et al., 1987; Weis et al., 1991a; McPhalen et al., 1991) were used in this analysis to detect any similarities to the KI domain sequences, using a database of known calcium binding motifs. The other aligned KI domains were also scanned for potential calcium binding motifs. The same procedure was applied for predicting the zinc binding motif within the KI domain by searching the sequence for a conserved arrangement of clustered histidines, methionines, and carboxylate residues (Christianson et al., 1991).

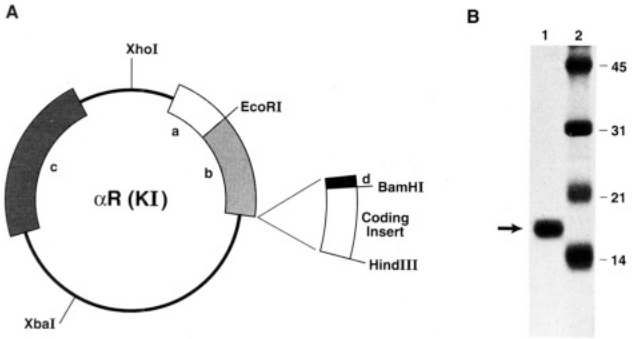

FIGURE 1: (A) Human α-PDGFR KI domain (104 residues) was synthesized using the PCR method, and the DNA insert was cloned into a pQE9 plasmid (type 4) (αRKI) (Qiagen). The vector possesses (*a*) a regulatable promoter/operator, (*b*) a synthetic ribosomal binding site RBSII, (*c*) β-lactamase, and (*d*) a six-histidine tag placed N-terminally. (B) pQE9 plasmid containing the DNA insert of the α-PDGFR KI domain was transfected into competent *M15 E. coli* cells, and gene expression was induced with 1.0 mM IPTG (isopropyl β-D-thiogalactopyranoside) for 4 h at 37 °C. The cells were spun down, and the protein was purified by denaturing conditions using Ni−NTA−agarose chromatography as described under Materials and Methods. The purified protein was eluted with 8 M urea, pH 5.9, and refolded by successive dialyses into either 50 mM Tris-HCl, pH 7.0, or 50 mM phosphate, pH 7.0. The purified KI domain was then electrophoretically separated on a 14% SDS−PAGE and stained with Coomassie blue.

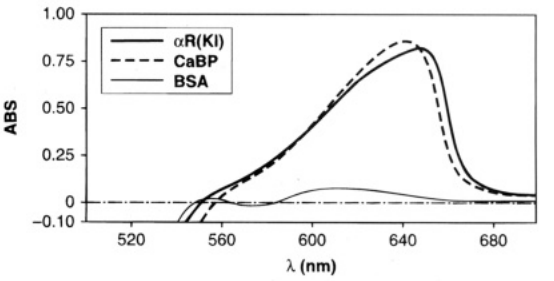

FIGURE 2: Stains-all binding to the native KI domain, vitamin D dependent calcium binding protein (CaBP), and bovine serum albumin (BSA) was measured in a solution containing 10 mM Tris base, pH 8.8, 0.001% Stains-all, and 0.1% formamide. The three proteins at a concentration of 10 μg were added to this solution and incubated for 30 min in the dark. The absorbance (ABS) was measured in the wavelength range 550−700 nm against a control solution containing only dye. (The KI domain is represented as a boldface line, CaBP as a dashed line, and BSA as thin line.)

RESULTS

Recombinant Expression and Purification of the α-PDGFR KI Domain. To study the structure of the α-PDGFR KI domain in relation to its known functions, we bacterially expressed and purified this domain. Figure 1A shows the expression vector pQE9 which contains an N-terminal six-histidine tag. Each liter of bacteria yielded 2−3 mg of protein. The purity of the preparation was estimated to be >95% by 14% SDS−PAGE following FPLC (MonoQ) (Pharmacia). The soluble, nonphosphorylated KI domain migrated at 16 kDa on SDS−PAGE (Figure 1B).

Stains-all Binding to Native Ca^{2+} Binding Proteins. Previously, we showed that the p85 N-SH2 domain binds calcium and this facilitated an interaction with the α-PDGFR in a calcium-dependent manner. However, this effect was in part due to the ability of the KI domain of the PDGFR to bind calcium ions (Mahadevan et al., 1994). In order to ascertain that the recombinant α-PDGFR KI domain binds calcium ions, "Stains-all" staining was performed. Vitamin D dependent calcium binding protein and bovine serum albumin as positive and negative controls were used, respectively. The results indicated that the addition of the KI domain and the vitamin D dependent calcium binding protein at the same concentration (10 μg) to the "Stains-all" solution turned the solution dark blue with a maximal absorbance in the wavelength range 620−640 nm, consistent with that observed for other calcium binding proteins (Campbell et al., 1983). Bovine serum albumin (10 μg) did not change color or absorb at 620−640 nm (Figure 2). Hence, the results clearly show that the α-PDGFR KI domain possesses a calcium binding site(s).

α-PDGFR KI Domain Has a Common Ca^{2+} and Zn^{2+} Binding Site. The $^{45}Ca^{2+}$ overlay provides a specific and sensitive method that allows the demonstration of high-affinity calcium binding sites within calcium binding proteins (see Materials and Methods). The α-PDGFR KI domain and the CaBP bound $^{45}Ca^{2+}$ at a concentration of 50 nM while the N-SH2 domain of GAP did not (Figure 3A). The p85 N-SH2 domain was not included in this experiment because it does not bind $^{45}Ca^{2+}$, but using indirect methods, we showed that it undergoes calcium-dependent conformational changes (Mahadevan et al., 1994). For the KI domain, unlabeled divalent and trivalent metal ions at 0.5 mM bound with the following rank order: $HO^{3+} = Zn^{2+} > Ni^{2+} > Ca^{2+} = Mn^{2+} > Mg^{2+}$, Ba^{2+}. Unlabeled Ho^{3+} and Zn^{2+} ions effectively competed out $^{45}Ca^{2+}$ (Figure 3B). However, unlabeled Ca^{2+} ions were not as effective as Ho^{3+} or Zn^{2+} ions but reduced the signal by 50%. Since Ho^{3+} ions can bind specifically to calcium binding proteins with higher affinity than calcium, this result suggests the presence of a calcium binding site within the KI domain. Further, the ability of Zn^{2+} ions to compete out $^{45}Ca^{2+}$ indicated the presence of a zinc binding site in the vicinity of the calcium binding site. Titration of $^{45}Ca^{2+}$ with unlabeled calcium chloride is shown (Figure 3C). The addition of 1 mM EGTA abolished the binding of $^{45}Ca^{2+}$ to the KI domain (data not shown), confirming that this domain has a calcium binding motif. The half-maximal value for binding calcium is 750 μM, indicating the presence of a low-affinity calcium binding site within the KI domain.

In order to ascertain that this domain directly binds zinc ions, a $^{65}Zn^{2+}$ study was performed after incubating (30 min at 4 °C) the KI domain with a saturating concentration of diethyl pyrocarbonate (DEPC), which is a histidine-modifying agent (Papini et al., 1989). The $^{65}Zn^{2+}$ signal was reduced by 50% in the DEPC-modified KI domain compared to the control (Figure 3D). Since 50% of $^{65}Zn^{2+}$ binding remained after DEPC modification, the KI domain could bind $^{65}Zn^{2+}$ through a histidine-independent site, located within its structure. To ensure that the remaining $^{65}Zn^{2+}$ bound to the α-PDGFR KI domain was not due to the ineffectiveness of DEPC to modify all histidine residues, we DEPC-treated the KI domain of colony stimulating factor-1 receptor (CSF-1R) (synthesized as a polyhistidine protein) to the same extent and detected no $^{65}Zn^{2+}$ binding. This finding suggests that the α-PDGFR KI domain possesses a Zn^{2+} binding site not dependent on histidine residues. A titration with unlabeled zinc ions provided a half-maximal value of 5 μM (Figure 3E). Further, the DEPC-modified protein bound $^{45}Ca^{2+}$ to the same extent as the unmodified protein, and unlabeled zinc chloride (0.5 mM) abolished this effect. These results suggest that the α-PDGFR KI domain possesses a common shared calcium and zinc binding site within its tertiary structure. It is well-known that calcium binding sites

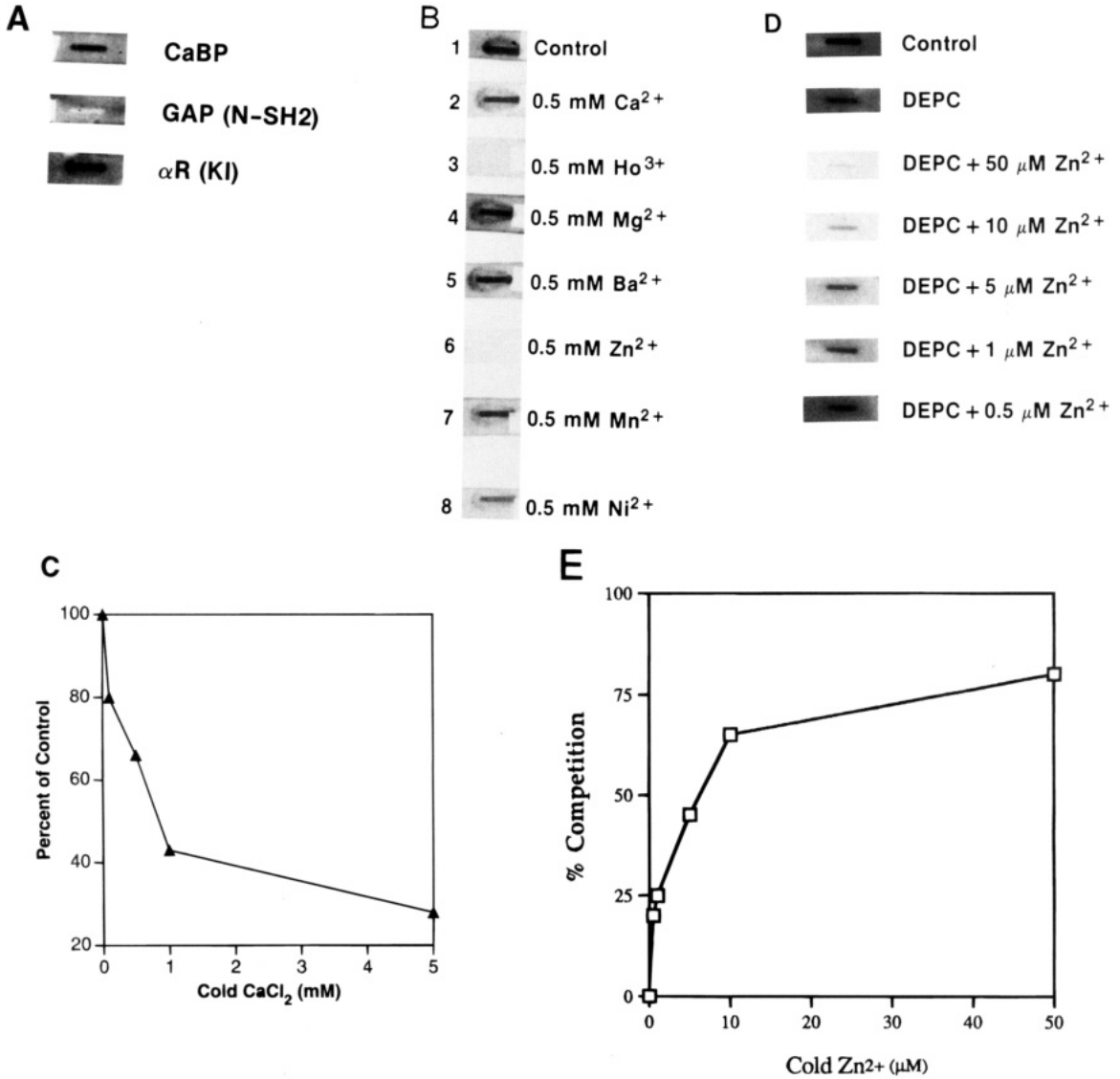

FIGURE 3: (A) Autoradiograph of a nitrocellulose slot blot with 2.5 μg of the KI domain incubated with $^{45}Ca^{2+}$ (see Materials and Methods). Vitamin D dependent calcium binding protein (CaBP) and the N-SH2 domain of GAP at a concentration of 2.5 μg are included as controls. (B) Competition of unlabeled divalent metal ions with $^{45}Ca^{2+}$. These experiments were performed in the absence or presence of 0.5 mM $CaCl_2$, $HoCl_3$, $ZnCl_2$, $BaCl_2$, $MnCl_2$, $MgCl_2$, and $NiCl_2$. (C) Titration of the competition of increasing amounts of unlabeled Ca^{2+} ions (0.1−5.0 mM) with $^{45}Ca^{2+}$. The autoradiograph was quantitated using a Phospho Imager (Molecular Dynamics), and the data are presented as the percent of the control against cold Ca^{2+} concentration. (D) Autoradiograph of a nitrocellulose slot blot with 2.5 μg of the KI domain and the DEPC-treated KI domain (DEPC modifies histidines) incubated with $^{65}Zn^{2+}$. The DEPC-modified KI domain shows a signal that is reduced by 50%, consistent with an internal zinc binding site that does not require histidines. (E) Titration of the competition of increasing amounts of unlabeled Zn^{2+} ions (0.5−50 μM) with $^{65}Zn^{2+}$. The autoradiograph (D) was quantitated, and the data are presented as the percent competition.

are acidic (McPhalen et al., 1991), while zinc binding sites requires the presence of at least two histidines or methionines or cysteines with one or two acidic amino acids (Christianson, 1991). Sequence analysis of the human α-PDGFR KI domain (discussed below) strongly suggests the presence of a common shared calcium and zinc binding site within its structure.

Conformational Changes Induced by Calcium and Zinc Ions in the α-PDGFR KI Domain Studied by Circular Dichroism Spectroscopy. Conformational changes in solution have been studied by circular dichroism spectroscopy for a variety of proteins. This method also provides a means of estimating protein secondary structure (Provencher & Glockner, 1981). The far-UV CD spectrum of the KI domain recorded in aqueous solution exhibited a trough at 205 nm and a smaller trough at 225 nm (Figure 4A), indicating the presence of both α-helix and β-sheet structure. The calculated secondary structure composition is 15% α-helix, 15% β-sheet, and 70% nonperiodic structure, which does not agree well with the secondary structure prediction (see below).

Since the KI domain binds both calcium and zinc ions, we studied whether these ions could induce conformational changes. The addition of calcium ions at 1 μM changed the conformation of this domain significantly. The protein lost more secondary structure on binding these metal ions as observed by the decrease in molar ellipticity. Further, additions (10, 100 μM) of calcium ions enhanced this effect, and a plateau was reached at 10 μM calcium (Figure 4A,C). The half-maximal value for a conformational change was 5 μM. The addition of zinc ions changed the CD spectrum marginally at 100 μM (Figure 4B). The $^{45}Ca^{2+}$ and $^{65}Zn^{2+}$ study indicated that the affinities of these ions for the KI domain are very different, zinc having an affinity 75-fold greater than calcium. However, conformational changes

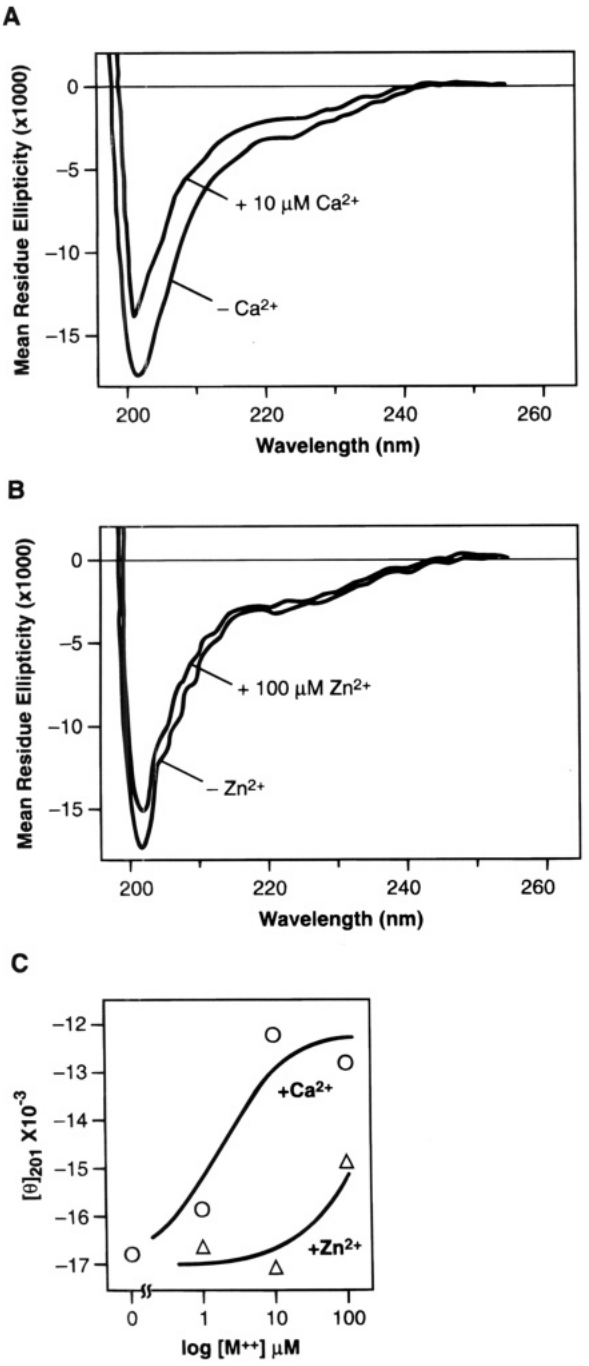

FIGURE 4: Far-UV CD spectrum of the purified KI domain (0.1 mg/mL) in 50 mM Tris-HCl buffer at pH 7.0 ($-Ca^{2+}$). Far-UV CD spectrum of the purified KI domain (0.1 mg/mL) in 50 mM Tris-HCl buffer, pH 7.0, in the presence of 10 μM calcium ($+Ca^{2+}$). (B) Far-UV CD spectra of the purified KI domain (0.1 mg/mL) in 50 mM Tris-HCl buffer, pH 7.0, in the presence of 100 μM zinc. (C) Titration of the conformational changes induced by calcium (○) and zinc (△) ions. The half-maximal value for calcium is 5 μM.

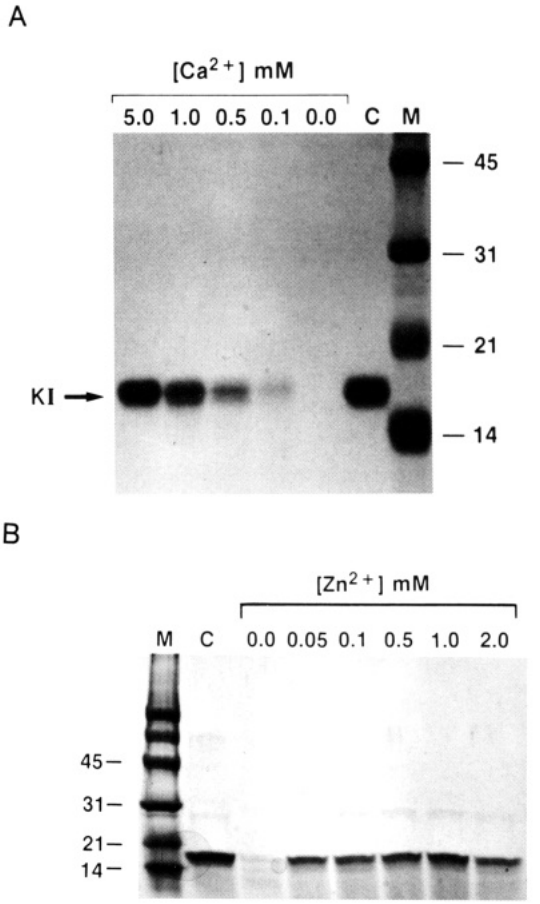

FIGURE 5: (A) KI domain (0.1 mg/mL) in 50 mM Tris-HCl, pH 7.0, was incubated with subtilisin (1 μg/mL) in the presence of increasing Ca^{2+} ion concentrations (0.0, 0.1, 0.5, 1.0, and 5.0 mM) for 5 min at 37 °C. The samples were then subjected to 14% SDS−PAGE analysis followed by staining with Coomassie blue. (B) KI domain (0.1 mg/mL) in 50 mM Tris-HCl, pH 7.0, was incubated with subtilisin (1 μg/mL) in the presence of increasing Zn^{2+} ion concentrations (0.0, 0.05, 0.1, 0.5, 1.0, and 2.0 mM) for 5 min at 37 °C. The samples were then subjected to 14% SDS−PAGE analysis followed by staining with Coomassie blue.

cannot be related to affinity in any rational way (McPhalen et al., 1991). Therefore, it can be postulated that the zinc binding site is preformed, while the calcium site is induced to form in the presence of calcium ions.

Calcium and Zinc Ions Differentially Protect KI Domain Proteolysis by Subtilisin. Limited proteolysis with subtilisin has been used to demonstrate the ability of divalent metal ions to protect metalloproteins from proteolytic digestion (Weis et al., 1991b; Mahadevan et al., 1994). Since the KI domain binds to both calcium and zinc ions, the limited proteolysis assay with subtilisin was employed to confirm this observation. Hence, the KI domain was incubated with subtilisin in the presence of varying amounts of calcium or zinc ions for either 5 or 10 min at 37 °C. Figure 5A,B shows that in the absence of calcium or zinc, the KI domain was not protected by subtilisin proteolysis. However, the addition of increasing concentrations of calcium or zinc resulted in a dose-dependent increase in protection of the KI domain from proteolysis (Figure 5A,B). The calcium and zinc ion concentrations required for reaching the half-maximal protease-resistant fraction were 1 and 0.6 mM, respectively. Hence, it may be concluded that zinc ions are better than calcium ions in protecting the KI domain from proteolysis. This is consistent with the $^{65}Zn^{2+}$ overlay which indicated a higher affinity of this ion for binding the KI domain. However, the conformation of the KI domain is significantly changed in the presence of calcium ions as measured by CD, and this changed conformation renders it resistant to proteolysis. It thus appears that the two metal ions protect the KI domain from proteolysis by different mechanisms: zinc binds the KI domain with a higher affinity but does not change its conformation, while calcium binds with a lower affinity and does change its conformation. However, both ions are protective with zinc being more effective than calcium. Since these metal ions confer protection, it can be surmised that the KI domain has a globular three-dimensional

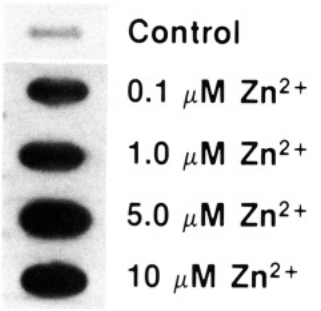

FIGURE 6: Identical amounts of the p85 N-SH2 domain (2.5 μg) were placed on nitrocellulose membranes via a slot blotter. The membranes were incubated with α-PDGFR (50 ng) in the absence and presence of increasing zinc ions (0.1−10 μM). The filters were washed and subjected to immunoblot analysis using anti-P-Tyr antibodies.

structure, as a random structure would be proteolyzed despite nonspecific metal binding.

Zinc Ions Enhance Association of the p85 N-SH2 Domain with Activated α-PDGFR. The binding of activated PDGFRs to p85 (PI-3K) and its SH2 domains has been examined by an *in vitro* binding assay (Kashishian et al., 1992; Mahadevan et al., 1994). This binding assay was employed to assess and quantitative whether zinc ions could stabilize the binding of the p85 N-SH2 domain to activated α-PDGFR. Purified p85 N-SH2 domain was immobilized on filters and incubated with the activated α-PDGFR in the absence and presence of zinc ions. Following incubation, filters were washed extensively and subjected to immunoblot analysis using anti-P-Tyr antibodies. The level of anti-P-Tyr-detectable α-PDGFR bound to the p85 N-SH2 domain was quantified. Figure 6 shows that in the absence of zinc ions, the association of the PDGFR with the p85 N-SH2 domain was weakly detectable. However, in the presence of increasing concentrations of zinc ions, the p85 N-SH2 domain association with the α-PDGFR increased 10−15-fold compared to the control. The half-maximal receptor binding for zinc was estimated to be approximately 0.5 μM (Figure 6). These findings suggest that divalent metal ions such as zinc specifically regulate the binding of the p85 N-SH2 domain to the activated α-PDGFR in a dose-dependent manner.

The Nonphosphorylated KI Domain Effectively Competes with the Activated α-PDGFR for p85 N-SH2 Domain Binding. In order to investigate the effect of divalent cations on PDGFR association with the p85 N-SH2 domain is mediated via the KI domain, association studies were performed in the presence of the KI domain. The results shown in Figure 7A quantitate the ability of the KI domain to compete with the baculovirus-expressed α-PDGFR for binding to the p85 N-SH2 domain in the absence and presence of Ca^{2+} ions. The addition of the KI domain (1−14 μM) in the presence of 0.5 mM calcium reduced the anti-P-Tyr signal and gave a half-maximal value for competition of 3.5 μM for the KI domain (Figure 7B). The data indicate that Ca^{2+} ions enhance the ability of the KI domain to compete with the α-PDGFR only when used at lower KI concentrations (0.5 μM). Since Mg^{2+}, Mn^{2+}, and ATP were absent, it can be argued that the α-PDGFR tyrosine kinase was unable to phosphorylate the KI domain and the observed competition was due to the effect of the nonphosphorylated KI domain. Incubation of the KI domain with anti-P-Tyr antibodies yielded no detectable signal, suggesting that the bacterially expressed material was not tyrosine-phosphor-

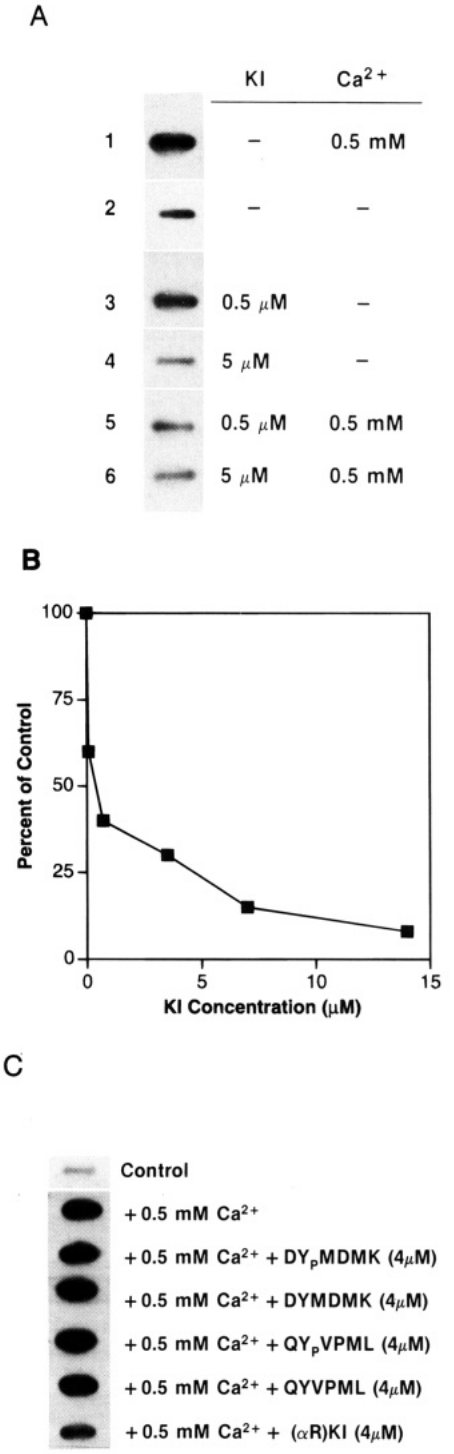

FIGURE 7: (A) Purified N-SH2 domain of p85 (2.5 μg) was immobilized onto a nitrocellulose membrane via a slot blotter. To measure binding *in vitro*, the baculovirus-activated α-PDGFR (75 ng) without ATP was incubated with 5 mL of binding assay buffer (50 mM Hepes at pH 7.0, 50 mM NaCl, and 0.1% Triton X-100) in the absence and presence of 0.5 mM Ca^{2+} ions for 1 h at room temperature. The membranes were washed and blotted with anti-P-Tyr antibodies. The KI domain at 0.5 and 5.0 μM was added to the above mixture in the absence and presence of 0.5 mM Ca^{2+} ions for 1 h at room temperature. The membranes were washed and blotted with anti-P-Tyr antibodies. (B) Quantitation of the competitive effect of the KI domain at increasing concentrations (1−14 μM) in the presence of 0.5 mM Ca^{2+} ions. The level of PDGFR binding was measured by scanning densitometry. (C) Effect of the peptides DYMDMK and QYVPML, phosphorylated and nonphosphorylated on the tyrosine, at a concentration of 4 μM compared with that of the KI domain (4 μM), for competition for the p85 N-SH2 domain binding in the presence of activated α-PDGFR.

ylated. Further, when the KI domain was incubated with the activated α-PDGFR and probed with anti-P-Tyr antibodies, a signal was not detectable, suggesting that the KI domain does not associate with the PDGFR. These data show that the observed effect was due to the ability of the KI domain to compete with the PDGFR for p85 N-SH2 binding.

Two hexapeptides (DYMDMK, QYVPML), one set nonphosphorylated and the other phosphorylated on the tyrosine, from the α-PDGFR KI domain which are thought to interact with the p85 SH2 domains were used to observe whether they could compete with α-PDGFR for binding the p85 N-SH2 domain. The nonphosphorylated and the phosphorylated peptides at a concentration 4 μM were not effective in competing with the α-PDGFR in the presence of calcium ions (Figure 7C). However, the KI domain at the same concentration reduced the signal by half (Figure 7B,C). Previous studies have shown that consensus peptide−SH2 interactions are in the nanomolar range (Fantl et al., 1992). However, recent binding studies indicate that the affinity of this interaction is around 40 μM (Bibbins et al., 1994). Our experiments are consistent with these results. Therefore, the inability of the consensus peptides to compete at 4 μM is likely to be due to their lower affinity interaction with the N-SH2 domain. The peptides at 40 μM were effective at competing with the PDGFR in the presence of 0.5 mM calcium chloride (data not shown). Taken together, these results support the notion that the nonphosphorylated KI domain is an effective competitor for p85 N-SH2 domain binding with that of the intact phosphorylated PDGFR. The peptides at molar equivalent concentrations used were ineffective, suggesting that the tertiary structure of the KI domain provides sufficient determinants for its association with SH2 domains and tyrosine phosphorylation may provide an additional mechanism for a more efficient interaction.

α-PDGFR KI Domain Delays Insulin-Induced GVBD in X. laevis Oocytes. The process of GVBD induced by insulin involves signaling pathways initiated by tyrosine phosphorylation of the oocyte receptor for this agonist. In contrast, progesterone-induced GVBD involves pathways dependent on the activation of adenylate cyclase triggered by progesterone at the oocyte surface. In order to determine whether the KI domain was in a biologically active conformation, we tested in *Xenopus* oocytes whether the microinjected KI domain affects the process of GVBD induced by insulin or progesterone. Figure 8 shows that the microinjection of oocytes with the KI domain produced a significant delay in the process of insulin-stimulated maturation (A) but had no effect on progesterone-induced maturation (B). The insulin-induced effect occurs in a concentration-dependent manner in that injection of one-third of the amount of the KI domain did not produce any measurable delay in insulin-induced maturation as compared to uninjected controls (data not shown). The microinjected hexapeptides (phosphorylated and nonphosphorylated) had no effect on GVBD (data not shown), suggesting that these peptides are not effective compared to the nonphosphorylated KI domain.

The KI Domain Is a Mixed α+β Protein. Multiple sequence alignments of protein families provide information on residue conservation and variability. Conserved residues generally are part of regular secondary structure, while variable residues are part of nonregular secondary structure (loops/turns) (Banga et al., 1990). Sequence alignment of the KI domains of the α- and β-PDGFRs, CSF-1R, flt, and

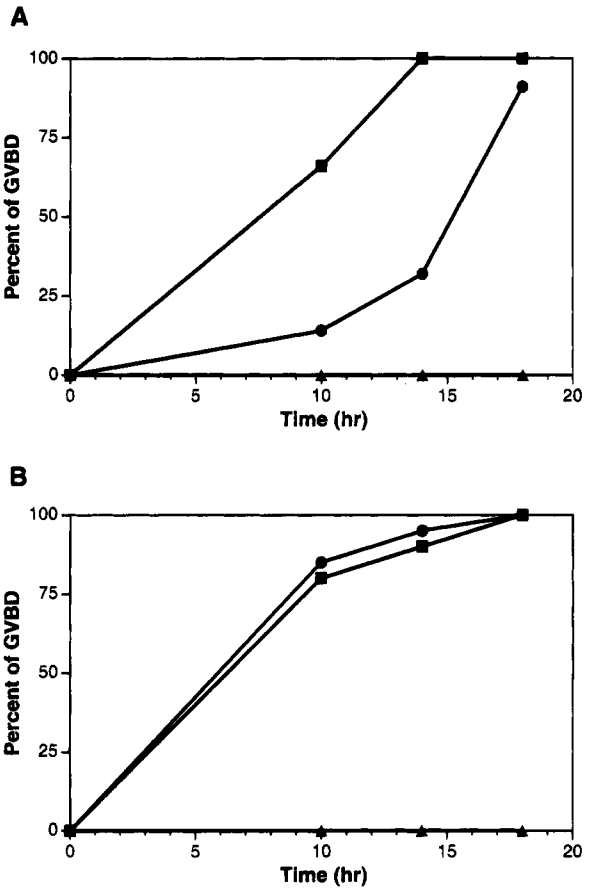

FIGURE 8: Time course of GVBD of *X. laevis* oocytes in the presence of (A) 7 μM insulin alone (■) and in the presence of 7 μM insulin with 90 ng of α-PDGFR KI domain microinjected (●). (B) The time course of GVBD in the presence of 15 μM progesterone alone (■) and in the presence of 15 μM progesterone with 90 ng of KI domain microinjected. The 20 mM Tris buffer, pH 7.5, alone is also shown (▲).

c-kit indicates that although the residue identity is not high the similarity is in the region of 25−30% and hence they are predicted to have similar secondary and tertiary structures (Figure 9). This domain is mainly acidic and hydrophilic. Specific phosphorylated tyrosines within the KI domain to which the SH2 domains of PI-3K (p85) and GAP bind are highlighted.

Secondary structure prediction methods are generally 65% accurate for a three-state prediction of helix, strand, and coil structures. Combined prediction methods can improve the accuracy, as can combining predictions on accurately aligned sequences (Zvelebil et al., 1987). Secondary structure predictions using the Leeds package which includes eight prediction methods were performed independently on each aligned sequence, and then the results were combined in a consensus. Figure 9 indicates the arrangement of the secondary structure elements along the polypeptide chain. The α-PDGFR KI domain is predicted to be a mixed α+β protein with 40% α-helix, 15% β-sheet, and 45% turns. However, CD spectroscopy (discussed above) indicated 15% α-helix, 15% β-sheet, and 70% turn conformation. For the β-PDGFR, CSF-1R, and v-kit KI domains, the prediction is in agreement with the CD data. The prediction for the flt KI domain is essentially β-sheet and turn with no α-helical contribution. Given the sequence diversity among the KI domains of the PDGFR subfamily, the predicted secondary structure for these domains is similar. This suggests that the tertiary structure is also conserved for these domains.

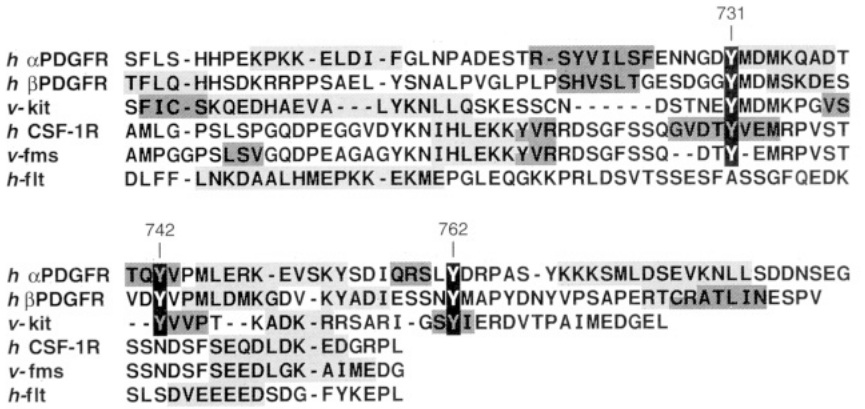

FIGURE 9: KI domains of the human α- and β-PDGFRs were aligned with those of human CSF-1R, flt, fms, and v-kit for maximum sequence similarity, including creation of gaps for insertions and deletions. The tyrosine residues thought to interact with the SH2 domains of p85 (Y731 and Y742) and GAP(Y771) are highlighted. The consensus secondary structure for each sequence is indicated by dark (β-sheet) and light (α-helix) shading. The prediction indicates a domain composed of α+β structure.

FIGURE 10: Sequence alignments of the human α- and β-PDGFR KI domains showing the shared potential Ca^{2+}/Zn^{2+} binding site. The human CSF-1R KI domain sequence is also aligned to show a potential Ca^{2+} binding site. The consensus secondary structure prediction for this region is indicated to be on a helix−turn−helix motif.

The Prediction of a Common Calcium and Zinc Binding Site within the KI Domain. The prediction of calcium or zinc binding sites within a protein structure is not straightforward. One method is to compare the sequence in question with already known calcium or zinc binding proteins to identify conserved primary and secondary structures. However, the $^{45}Ca^{2+}/^{65}Zn^{2+}$ study clearly indicates that the divalent metal binding site within the KI domain is shared. This makes it easier to predict accurately the "common" binding site because calcium and zinc ions require preferred ligands.

A scan of the α-PDGFR KI domain sequence revealed a potential metal ion binding site that could satisfy both calcium and zinc ions. This site encompasses the tyrosine phosphorylation sites (Tyr731,742) that interact with the SH2 domains of PI-3K (p85). Three methionines (Met732,734,745) and four carboxylates (Asp730,733,738 and Glu747) clustered in this region are predicted to be the common calcium/zinc binding site (Figure 10). Secondary structure prediction indicates the proposed metal binding site to be on a helix−loop−helix, consistent with structural data. From a sequence comparison, it is also predicted that the β-PDGFR KI domain also possesses a common calcium/zinc binding site, while the CSF-1R KI domain is predicted to possess a calcium binding site but not a zinc binding site. This prediction has been confirmed by further analysis (data not shown).

DISCUSSION

The PDGFR subfamily of receptors possesses a kinase insert domain (KI) of about 100 residues which interrupts the 2-domain tyrosine kinase. The α- and β-PDGFR KI domains are autophosphorylated on several tyrosine residues which form the binding sites for the SH2 domains of PI-3K (p85) and GAP. Site-directed mutagenesis and deletion/substitution mutagenesis studies of the α- and β-PDGFR KI domains showed reduced or abolished biochemical and mitogenic effects. The evolution of a KI domain within the receptor tyrosine kinases may have a functional advantage in that the binding of signaling proteins to this domain may provide efficient access for tyrosine phosphorylation by the kinase and allows the activation of multiple signaling pathways with a degree of redundancy.

In order to probe structure in relation to function, we bacterially expressed and purified the nonphosphorylated α-PDGFR KI domain. It was previously shown that the p85 C-SH2 domain bound the β-PDGFR with an affinity 100-fold higher than the N-SH2 domain (Klippel et al., 1992). However, in contrast, Kavanaugh et al. (1992) showed that the p85 N-SH2 domain bound the β-PDGFR but the C-SH2 domain did not. Although the reasons underlying this disparity have not been resolved, McGlade et al. (1992) have shown that both SH2 domains of p85 bound with similar efficiencies to the β-PDGFR and the EGFR. Since accumulating evidence suggests that both N- and C-SH2 domains are functionally similar, we chose the N-SH2 domain to study its interaction with the α-PDGFR. Consistent with these findings, we showed that the N-SH2 domain associated with the β-PDGFR independent of Ca^{2+} ions. However, under these conditions, the binding of the N-SH2 domain to the α-PDGFR was shown to depend on Ca^{2+} ions (Mahadevan et al., 1994). These results led us to conclude that (1) the calcium-mediated binding of the N-SH2 domain to the α-PDGFR and (2) the calcium effect were not just due to the N-SH2 domain but also to the kinase insert domain of the α-PDGFR. This suggested that the KI domain also had the capability of binding calcium ions. The cationic dye "Stains-all" that binds to calcium sites within calcium binding proteins bound the KI domain to a similar extent to that of vitamin D dependent calcium binding protein (CaBP). The $^{45}Ca^{2+}$ overlay confirmed this conclusion (K_D = 750 μM). The $^{45}Ca^{2+}$ study also indicated that unlabeled zinc ions competed with calcium for binding the KI domain, which strongly suggested a common divalent metal ion binding site. The $^{65}Zn^{2+}$ overlay confirmed the presence of a zinc binding site within this domain (K_D = 5.0 μM). The binding of calcium ions to the KI domain changed its conformation significantly (half-maximal value of 5 μM in CD), and this changed conformation was resistant to sub-

tilisin proteolysis. However, zinc ions at 100 μM only marginally affected the conformation but were more efficient in protecting this domain from subtilisin proteolysis. It appears that Zn^{2+} ion binding to the KI domain modifies the site of proteolysis without significantly altering the conformational changes measured by CD spectroscopy. The subtilisin proteolysis study clearly indicates the KI domain to have a globular tertiary structure which is stabilized by Ca^{2+} and Zn^{2+} ions.

Multiple sequence alignment of the KI domains of the PDGFR subfamily receptors (α- and β-PDGFR, CSF-1R, c-kit, flt) was performed for sequence homology, secondary structure prediction, and rationalization of divalent metal ion binding site(s). The percent identity and similarity were 20% and 40%, respectively, suggesting a similar overall tertiary structure for these domains. Although the KI domains of CSF-1R, c−kit, and flt are 25% shorter than the PDGFR KI domains, they are also predicted to have a similar tertiary structure. The consensus secondary structure prediction of the α-PDGFR KI domain differed from that estimated by CD spectroscopy. The prediction overestimated the regular secondary structural elements, while CD indicated a domain consisting of 15% α-helix, 15% β-sheet, and 70% nonperiodic structure. However, despite the low percentage of regular secondary structure, this domain is an independently folded globular structure, as ascertained by subtilisin proteolysis. Sequence alignments strongly suggested that for the α-PDGFR KI domain the region encompassing the p85 N-SH2 domain binding site possessed an area rich in methionines (Met732,734,745) and carboxylic acids (Asp730,-733,738 and Glu747), which could support a common Ca^{2+}/Zn^{2+} binding site. The secondary structure predicted for this region was helix−turn−helix, commonly observed as structural elements for Ca^{2+}/Zn^{2+} sites within proteins. Further, it is also predicted that the β-PDGFR KI domain also possesses a common Ca^{2+}/Zn^{2+} binding site, while the CSF-1R KI possesses only a calcium binding site. There are examples of cellular calcium binding proteins such as calreticulin (CRT) and calsequestrin (CS) which have sites for calcium and zinc ions (Heilmann et al., 1993), and this suggests that the KI domains within the PDGFR subfamily may use metal binding for both structural stability and functional efficiency. Unlike for calcium ions, there are sparse data on cellular concentrations of zinc ions, but in rat liver, the cytosolic zinc levels have been estimated at 200−500 μM (Brand et al., 1988).

The physiological significance of zinc ions to the functions of the PDGFR is unknown. It may be postulated that the zinc ions provide structural stability to the KI domains of the PDGFRs, allowing the SH2 domains of p85 and possibly GAP to bind with high affinity. The binding of the p85 N-SH2 domain to the α-PDGFR is markedly enhanced in the presence of Zn^{2+} ions with a half-maximal value of 0.5 μM. A similar effect was observed with Ca^{2+} ions (Mahadevan et al., 1994) but with a half-maximal value of 25 μM. It has been shown that the Ca^{2+} ion concentration can vary markedly within cells, sometimes reaching 1 mM levels. Such localized levels have been observed close to the plasma membrane (Murachi, 1989). Therefore, it can be postulated that in the presence of calcium spikes, the α-PDGFR binds Ca^{2+} ions and enhances p85 N-SH2 domain association. At other times, the p85 N-SH2 domain may be associated with the PDGFR through a Zn^{2+} ion dependent mechanism.

The α-PDGFR KI domain in the presence of calcium ions is able to compete effectively with the activated α-PDGFR for binding the N-SH2 domain of p85. Hence, it may be postulated that in the presence of calcium ions the KI domain binds the p85 N-SH2 domain. We have shown that this association does indeed occur in an *in vitro* binding assay (Mahadevan, unpublished data). The nonphosphorylated KI domain was able to compete with the activated α-PDGFR for SH2 domain binding in the presence of calcium ions with a K_D value of 3.5 μM. Since the nonphosphorylated KI domain also binds calcium and in the same region as the SH2 domain, it appears that calcium ions modulate SH2−PDGFR interactions, through their tyrosine binding sites (Y740, 751). It may be postulated that calcium ions perform a dual function, in that they bind to both SH2 and KI domains, changing their conformation sufficiently such that efficient binding occurs. Since the intracellular calcium ion concentration varies significantly (Berridge, 1993), this effect is optimized during calcium spikes.

Phosphotyrosine-dependent (Yu et al., 1991; Fantl et al., 1992; Kashishian et al., 1992) and -independent binding of SH2 domains has previously been demonstrated (Cooper & Kashishian, 1993; Pendergast et al., 1991). Recently, the wild-type Src SH2 domain was shown to bind a 13-residue peptide from the β-PDGFR KI domain incorporating Y751 (PD 751) (Bibbins et al., 1993). Further, the mutant R175L SH2 domain displayed higher affinity for this nonphosphorylated peptide than other phosphopeptides (Bibbins et al., 1993). We are also able to show that the nonphosphorylated KI domain is able to associate with the p85 N-SH2 domain in the absence of calcium and this effect is markedly enhanced in the presence of calcium ions (Mahadevan et al., unpublished results). However, the two tyrosine-phosphorylated hexapeptides were only able to compete with the PDGFR at a K_D value of 40 μM even in the presence of calcium ions. Hence, it appears that at least for some SH2 domains binding may be phosphotyrosine-independent. This observation is supported by the R155K and R155A mutations which only reduce binding to phosphotyrosine peptides slightly (Bibbins et al., 1993). Interestingly, R155 in the Src SH2 crystal structure is shown to be important in the recognition of the phosphate group and the aromatic ring of the tyrosine (Waksman et al., 1993). Bibbins et al. (1993) have analyzed this possibility in light of an acidic residue at the −3 or −4 position with respect to the phosphotyrosine. A single change of this acidic residue to an alanine decreased the affinity for SH2 binding. The region N-terminal to the phosphotyrosine was not previously considered an important factor in SH2 domain recognition. Since the KI domain is an independently folded globular domain, it possesses the structural features required for SH2 domain binding and thus supports the above observations.

PDGFR and IRS-1 have been shown to physically associate with the p85 N-SH2 domain in a tyrosine phosphorylation-dependent manner (Backer et al., 1992). Microinjection studies with *Xenopus* oocytes with IRS-1 (Chuang et al., 1993a) and the p85 N-SH2 domain (Chuang et al., 1993b) have shown that insulin promotes GVBD by phosphorylating IRS-1 and this effect is inhibited by the p85 N-SH2 domain by preventing PI-3K activity. IRS-1 contains 21 potential tyrosine phosphorylation sites, including 6 in YMXM motifs, 3 in YXXM motifs, and 12 other hydrophobic motifs. At least eight tyrosines undergo phosphorylation by the activated insulin receptor, four of which have the YMXM motif (White

& Kahn, 1994). The p85 N-SH2 domain binds through the YMXM motif, and this is also present on the α-PDGFR KI domain. In order to investigate whether the KI domain was in a biologically active conformation, this domain was microinjected into *Xenopus* oocytes, and in the presence of insulin, GVBD was significantly delayed, but this effect was not observed in the presence of progesterone. This observation is consistent with the fact that nonphosphorylated KI domain has the ability to bind the p85 N-SH2 domain by a tyrosine phosphate independent mechanism. However, the hexapeptides (tyrosine phospho- and nonphospho-) microinjected into *Xenopus* oocytes showed no effect on GVBD in the presence of insulin, suggesting that IRS-1 was capable of overcoming their potential inhibitory effects. IRS-1 can bind other SH2 domains (Grb 2, SHPTP-2, and Nck) through distinct sites to that of the p85 N-SH2 domain. The PDGFR KI domain has also been shown to associate with SH2 domains p85 and Nck and may be competing with these proteins for binding IRS-1 and other interacting signaling proteins.

In conclusion, we have shown that the α-PDGFR KI domain possesses a novel divalent metal ion binding site that may help in association with the SH2 domains of PI-3K-(p85), thus regulating its activity *in vivo*.

ACKNOWLEDGMENT

D.M. dedicates this paper to John Abbott. We thank Dr. Steven Tronick for support and encouragement. We also thank Robert Wheelock for his technical help.

REFERENCES

Backer, J. M., Myers, M. G., Shoelson, S. E., Chin, D. J., Sun, X.-J., Miralpeix, M., Hu, P., Margolis, B., Skolnik, E. Y., Schlessinger, J., & White, M. F. (1992) *EMBO J. 11*, 3469−3479.

Banga, P., Mahadevan, D., Barton, G., Sutton, B., Saldanha, J., Odell, E., & McGregor, A. M. (1990) *FEBS Lett. 266*, 133−141.

Bazenet, C. E., & Kazlauskas, A. (1993) *Oncogene 9*, 517−525.

Berridge, M. J. (1993) *Nature 361*, 315−325.

Bibbins, K. B., Boeuf, H., & Varmus, H. E. (1993) *Mol. Cell. Biol. 13*, 7278−7287.

Bossemeyer, D., Engh, R. A., Kinzel, V., Ponstingl, H., & Huber, R. (1993) *EMBO J. 12*, 849−859.

Brand, I. A., Heinickel, A., Kratzin, H., & Soling, H.-D. (1988) *Eur. J. Biochem. 177*, 561−568.

Burgess, A. W., Ponnuswamy, P. K., & Scheraga, H. A. (1974) *Isr. J. Chem. 12*, 239−286.

Campbell, K. P., MacLennan, D. H., & Jorgensen, A. O. (1983) *J. Biol. Chem. 258*, 11267−11273.

Cantley, L. C., Auger, K. R., Carpenter, C., Duckworth, B., Graziani, A., Kapeller, R., & Soltoff, S. (1991) *Cell 64*, 281−302.

Chang, C. T., Wu, C. S. C., & Yang, J. T. (1978) *Anal. Biochem. 91*, 13−31.

Chou, P. Y., & Fasman, G. D. (1974) *Biochemistry 13*, 225−245.

Christianson, D. W. (1991) *Adv. Protein Chem. 42*, 281−355.

Chuang, L.-M., Myers, M. G., Seidner, G. A., Birnbaum, M. J., White, M. F., & Kahn, C. R. (1993a) *Proc. Natl. Acad. Sci. U.S.A. 90*, 5172−5175.

Chuang, L.-M., Myers, M. G., Backer, J. M., Shoelson, S. E., White, M. J., Birnbaum, M. J., & Kahn, C. R. (1993b) *Mol. Cell. Biol. 13*, 6653−6660.

Cooper, J. A., & Kashishian, A. (1993) *Mol. Cell. Biol. 13*, 1737−1745.

Dufton, M. J., & Hider, R. C. (1977) *J. Mol. Biol. 115*, 177−193.

Eliopoulis, E. E., Geddes, A. J., Brett, M., Pappin, D. J. C., & Findlay, J. B. C. (1982) *Int. J. Biol. Macromol. 4*, 263−267.

Escobedo, J. A., & Williams, L. T. (1988) *Nature (London) 335*, 85−87.

Escobedo, J., Kaplan, D. R., Kavanaugh, W. M., Turke, C. W., & Williams, L. T. (1991) *Mol. Cell. Biol. 11*, 1125−1132.

Fantl, W. J., Escobedo, J. A., Martin, G. A., Turck, C. W., del Rosario, M., McCormick, F., & Williams, L. T. (1992) *Cell 69*, 413−423.

Gailit, J., & Ruoslahti, E. (1988) *J. Biol. Chem. 263*, 12927−12932.

Garnier, J., Osguthorpe, D. J., & Robson, B. (1978) *J. Mol. Biol. 120*, 97−120.

Hanks, S. K., & Quinn, A. M. (1991) *Methods Enzymol. 200*, 38−81.

Heidaran, M. A., Pierce, J. H., Lombardi, D., Ruggiero, M., Gutkind, S. J., Matsui, T., & Aaronson, S. A. (1991) *Mol. Cell. Biol. 11*, 134−142.

Heidaran, M. A., Beeler, J. F., Yu, J.-C., Ishibashi, T., LaRochelle, W. J., Pierce, J. H., & Aaronson, S. A. (1993) *J. Biol. Chem. 268*, 9287−9295.

Heilmann, C., Spamer, C., Leberer, E., Gerok, W., & Michalak, M. (1993) *Biochem. Biophys. Res. Commun. 193*, 611−616.

Heldin, C.-H. (1992) *EMBO J. 11*, 4251−4259.

Heldin, C.-H., & Westermark, B. (1990) *Cell Regul. 1*, 555−566.

Jensen, R. A., Beeler, J. F., Heidaran, M. A., & La Rochelle, W. J. (1992) *Biochemistry 31*, 10887−10892.

Joly, M., Kazlauskas, A., Fay, F. S., & Corvera, S. (1994) *Science 263*, 684−686.

Kashishian, A., Kazlaukus, A., & Cooper, J. A. (1992) *EMBO J. 11*, 1373−1382.

Kavanaugh, W., Klippel, A., Escobedo, J., & Williams, L. (1992) *Mol. Cell. Biol. 12*, 3415−3424.

Kawasaki, H., Kasai, H., & Okuyama, T. (1985) *Anal. Biochem. 148*, 297−302.

Klippel, A., Escobedo, J., Fantl, W., & Williams, L. (1992) *Mol. Cell. Biol. 12*, 1451−1459.

Knighton, D. R., Zheng, J., Ten Eyck, L. F., Ashford, V. A., Xuong, N.-H., Taylor, S. S., & Sowadski, J. M. (1991a) *Science 253*, 407−413.

Knighton, D. R., Zheng, J., Ten Eyck, L. F., Xuong, N.-H., Taylor, S. S., & Sowadski, J. M. (1991b) *Science 253*, 414−420.

Koch, C. A., Anderson, D., Moran, M. F., Ellis, C., & Pawson, T. (1991) *Science 252*, 668−674.

Kretsinger, R. H. (1980) *CRC Crit. Rev. Biochem. 8*, 119−174.

Kundra, V., Escobedo, J. A., Kazlauskas, A., Kim, H. K., Rhee, S. G., Williams, L. T., & Zetter, B. R. (1994) *Nature (London) 367*, 474−476.

Lim, V. I. (1974) *J. Mol. Biol. 88*, 873−894.

Mahadevan, D., Thanki, N., McPhie, P., Beeler, J. F., Yu, J.-C., Wlodawer, A., & Heidaran, M. A. (1994) *Biochemistry 33*, 746−754.

Maruyama, K., Mikawa, T., & Ebashi, S. (1984) *J. Biochem. 95*, 511−519.

McGlade, C., Ellis, C., Reedijk, M., Anderson, D., Mbamalu, G., Reith, A., Panayotou, G., End, P., Bernstein, A., Kazlauskas, A., Waterfield, M., & Pawson, T. (1992) *Mol. Cell. Biol. 12*, 991−997.

McPhalen, C. A., Strynadka, N. C., & James, M. N. G. (1991) *Adv. Protein Chem. 42*, 77−144.

Morrison, D. K., Kaplan, D. R., Rhee, S. G., & Williams, L. T. (1990) *Mol. Cell. Biol. 10*, 2359−2366.

Murachi, T. (1989) *Biochem. Int. 18*, 263−294.

Nagano, K. (1973) *J. Mol. Biol. 75*, 401−420.

Papini, E., Schiavo, G., Sandona, D., Rappuoli, R., & Montecucco, C. (1989) *J. Biol. Chem. 264*, 12385−12388.

Pendergast, A. M., Muller, A. J., Havlik, M. H., Marn, Y., & Witte, O. N. (1991) *Cell 66*, 161−171.

Provencher, S. W., & Glockner, J. (1981) *Biochemistry 20*, 33−37.

Severinsson, L., Ek, B., Mellstrom, K., Claesson-Welsh, L., & Heldin, C.-H. (1990) *Mol. Cell. Biol. 10*, 801−809.

Shurtleff, S. A., Downing, J. R., Rock, C. O., Hawkins, S. A., Roussel, M. F., & Sherr, C. J. (1990) *EMBO J. 9*, 2415−2421.

Songyang, Z., Shoelson, S. E., Chaudhuri, M., Gish, G., Pawson, T., Haser, W. G., King, F., Roberts, T., Ratnofsky, S., Lechleider, R. J., Neel, B. G., Birge, R. B., Fajardo, J. E., Chou, M. M., Hanafusa, H., Schaffhausen, B., & Cantley, L. C. (1993) *Cell 72*, 767−778.

Sun, X.-J., Rothenberg, P., Kahn, R. C., Backer, J. M., Araki, E., Wilden, P. A., Cahill, D. A., Goldstein, B. J., & White, M. F. (1991) *Nature 352*, 73−77.

Taylor, G. R., Reedjik, M., Rothwell, W., Rohrschneider, L., & Pawson, T. (1989) *EMBO J. 8*, 2029−2037.

Ullrich, A., & Schlessinger, J. (1990) *Cell 61*, 203−212.

Vyas, N. K., Vyas, M. N., & Quiocho, F. A. (1987) *Nature 327*, 635−638.

Waksman, G., Shoelson, E. S., Pant, N., Cowburn, D., & Kuriyan, J. (1993) *Cell 72*, 779−790.

Weis, W. I., Crichlow, G. V., Krishna Murthy, H. M., Hendrickson, W. A., & Drickamer, K. (1991a) *J. Biol. Chem. 266*, 20678−20686.

Weis, W. I., Kahn, R., Fourme, R., Drickamer, K., & Hendrickson, W. A. (1991b) *Science 254*, 1608−1615.

Wennstrom, S., Siegbahn, A., Yokote, K., Arvidsson, A.-K., Heldin, C.-H., Mori, S., & Claesson-Welsh, L. (1994) *Oncogene 9*, 651−660.

White, M. F., & Kahn, R. C. (1994) *J. Biol. Chem. 269*, 1−4.

Yarden, Y., Escobedo, J. A., Kuang, W. J., Yang-Feng, T. L., Daniel, T. O., Tremble, P. M., Chen, E. Y., Ando, M. E., Hartkins, R. N., Francke, U., Friend, V. A., Ullrich, A., & Williams, L. T. (1986) *Nature 323*, 226−232.

Yu, J.-C., Heidaran, M. A., Pierce, J., Gutkind, J., Ruggiero, M., & Aaronson, S. A. (1991) *Mol. Cell. Biol. 11*, 3780−3785.

Zvelebil, M. J. J., Barton, G., Taylor, W., & Sternberg, M. (1987) *J. Mol. Biol. 195*, 957−961.

BI941736+